area for EXAFS. Many "real" problems provide experimental difficulties in gaining the long (>1 keV) data ranges with good signal-to-noise ratio necessary for such assessments.

A summary of the structural models and parameters used in fitting the EXAFS spectra of the supported species is shown in Chart I. Determination of interatomic distances, coordination numbers, and bond angles allows for a more detailed structural analysis of **2**, **3**, **4**, **5**, and **6** than has previously been obtained. Information on the M–O(surface) interaction is of particular interest as it is believed to play an important role in determining catalytic activity and selectivity for ultra-dispersed supported metals.

Distance determinations from the EXAFS data are reliable and accurate in contrast to the determination of occupation numbers. The values of N(M–O(surface)) obtained for **2**, **3**, **4**, and **5** would appear to be unrealistically high. It is felt that this is a result of large (probably) static disorders and high correlations between parameters. The nonideal nature of the interaction between mononuclear metal complexes or small metal clusters attached to the bulk of an oxide surface would therefore appear to present problems for accurate occupation number determination.

The incongruity between the IR data and determination of M–C–O bond angles by EXAFS suggests that a systematic error is involved in the determination of this parameter, which may also be due to the treatment of disorder as due to a single, isotropic factor.

Acknowledgment. We wish to thank SERC for a research studentship (R.J.P.), a research assistantship (N.B.), and use of the Daresbury Laboratory facilities. We also thank Johnson Matthey and Degussa for the ruthenium chloride and oxide samples, respectively.

Registry No. $Rh(CO)_{12}$, 19584-30-6; $Ru(CO)_{12}$, 15243-33-1; Al_2O_3, 1344-28-1; SiO_2, 7631-86-9.

Spectroscopic and Electrochemical Study of Trinuclear Ferracyclopentadienyl Clusters $[Fe_3(\mu\text{-}CO)_2(CO)_6(RC_2R)_2]$

Domenico Osella,* Giuseppina Arman, Mauro Botta, and Roberto Gobetto

Dipartimento di Chimica Inorganica, Chimica Fisica e Chimica dei Materiali, Università di Torino, Via Pietro Giuria 7, 10125 Torino, Italy

Franco Laschi and Piero Zanello*

Dipartimento di Chimica, Università di Siena, 53100 Siena, Italy

Received May 6, 1988

The redox chemistry of triiron metallacyclopentadienyl clusters $Fe_3(CO)_8(RC_2R)_2$ has been investigated by electrochemical and spectroscopic techniques. Their ^1H and ^{13}CNMR resonances have been assigned by comparison of the NMR data of different isomers and by two-dimensional and selective decoupling experiments. The sequence of electrode processes has been postulated on the basis of the response of cyclic voltammetry (CV), coulometry, electron spin resonance (ESR) spectroscopy, and chemical tests. The influence of the metallacyclopentadienyl ring substituents on the trend of the redox potentials supports the high electronic delocalization in the Fe_3C_4 skeleton previously postulated on the basis of theoretical calculations. Finally, an effective electron transfer catalyzed (ETC) synthesis of the two $[Fe_3(CO)_7P(OMe)_3(PhC_2Ph)_2]$ isomers has been achieved.

Introduction

Acetylene metal cluster compounds show a variety of structural arrangements that are suitable models for chemisorbed hydrocarbons on metallic surfaces.[1] It was recognized some time ago that the major products in the reactions between iron carbonyls and alkynes are complexes of the type $Fe_3(CO)_8(alkyne)_2$.[2,3] Such systems, which contain a ferracyclopentadienyl ring, are quite common in organometallic chemistry and have been considered as intermediates in the cyclotrimerization of alkynes.[4]

An X-ray structure study of $Fe_3(CO)_8(PhC_2Ph)_2$ (**1**) has been reported by Dodge et al.:[5] the metallic framework consists of an open triangle whose two edges are asymmetrically bridged by CO's and in which the metallacycle plane intersects the Fe_3 plane perpendicularly; the phenyl groups are twisted away from the FeC_4 plane in the same sense, all by about 55°. Two ^{13}C NMR studies have shown that this structural arrangement is maintained in solution and that CO ligands exchange locally on each Fe′ atom.[6,7] The electronic structure of molecules containing a pentaatomic metallacycle has received considerable attention since Hoffmann et al.[8] suggested that polynuclear metallacyclopentadienyl compounds are suitable candidates to exhibit a six-π-electron aromaticity. Combined UV–PES

(1) (a) Ugo, R. *Catal. Rev.* **1975**, *11*, 225. (b) Muetterties, E. L.; Rhodin, T. N.; Bond, E.; Brucker, C. F.; Pretzer, W. R. *Chem. Rev.* **1979**, *79*, 91.
(2) Hubel, W. In *Organic Syntheses via Metal Carbonyls*; Wender, I., Pino, P., Eds.; Wiley-Interscience: New York, 1968.
(3) Fehlhammer, W. R.; Stolzenberg, H. In *Comprehensive Organometallic Chemistry*; Wilkinson, G., Stone, F. G. A., Abel, E. W., Eds.; Pergamon: Oxford, 1982.
(4) Vollhardt, K. P. C. *Acc. Chem. Res.* **1977**, *10*, 1.
(5) Dodge, R. P.; Schomaker, V. *J. Organomet. Chem.* **1965**, *3*, 274.
(6) Hickey, J. P.; Wilkinson, J. R.; Todd, L. J. *J. Organomet. Chem.* **1975**, *99*, 281.
(7) Aime, S.; Milone, L.; Sappa, E. *Inorg. Chim. Acta* **1976**, *16*, L7.
(8) Thorn, D. L.; Hoffmann, R. *Nouv. J. Chim.* **1979**, *3*, 39.

0276-7333/89/2308-0620$01.50/0

and theoretical (ab initio and DV–Xα) calculations have been performed on $M_2(CO)_6(RC_2R)_2$ and $M_3(CO)_8(RC_2R)_2$ (M = Fe, Ru, Os) derivatives.[9,10] In the polyhedral skeletal electron pair (PSEP) approach, developed by Wade and Mingos,[11] $Fe_3(CO)_8(RC_2R)_2$ systems are expected to assume a closo pentagonal-bipyramidal geometry [S (skeletal electron pairs) = 8, n (skeletal atoms) = 7]. Their thermal decomposition to $Fe_2(CO)_6(RC_2R)_2$ homologues is accounted for by elimination of an apical "$Fe(CO)_2$" fragment (S = 0) to give the corresponding nido pentagonal-bipyramidal structure (S = 8, n = 6), a sort of cluster-contraction reaction. This reaction can be reversed to some extent by refluxing the binuclear derivatives with $Fe_2(CO)_9$ (a suitable source of "$Fe(CO)_2$" fragments in solution[12]); the equilibrium depends on the steric encumbrance of the alkyne substituents.[13]

We have been interested in the electrochemistry of organometal clusters, a recent aspect of their chemistry that may offer a clue for their efficient and selective electrosyntheses. The extensive σ/π interactions occurring between the organic fragment and the metallic frame usually improve the stability of the electrogenerated ionic species with respect to the parent binary carbonyls. This is the case of $Co_3(CO)_9(\mu_3\text{-}CY)$[14] (Y = halogen, alkyl, or aryl substituent), $HRu_3(CO)_9(\mu_3\text{-}CR)$[15] (R = allyl, allenyl, or acetylido radical), $Fe_3(CO)_9$(alkyne),[16] and $Fe_2(CO)_6$[(alkyne)$_2$CO][17] derivatives. The reversible redox sequences in these organometal clusters allow one to extract interesting electronic and thermodynamic information.[18] This is almost certainly the case of $Fe_3(CO)_8$(alkyne)$_2$ systems, since highly delocalized orbitals are predicted by theoretical calculations.[9] Moreover, a brief report on the electrochemical features of $Fe_3(CO)_8(PhC_2Ph)_2$ (**1**) (among hundreds of other organometallic compounds) has been published by Dessy et al.[19] and has indicated a reversible redox behavior. In order to test the hyphothesis of electronic delocalization in the title compounds and in order to assess the influence of the alkyne substituents on the electrochemistry, we have optimized stepwise syntheses of a large number of $Fe_3(CO)_8$(alkyne)$_2$ derivatives and carried out a systematic NMR and electrochemical study on them.

Results and Discussion

Syntheses and Characterization of Trinuclear Metallacyclopentadienyl Derivatives. The reaction sequence that affords the $Fe_3(CO)_8(RC_2R)_2$ compounds and their thermal decomposition products, the binuclear $Fe_2(CO)_6(RC_2R)_2$ homologues, has been clearly established by Hubel et al.[2] with the aid of X-ray determinations carried out by Dahl,[20] Dodge,[5] Hock,[21] and co-workers.

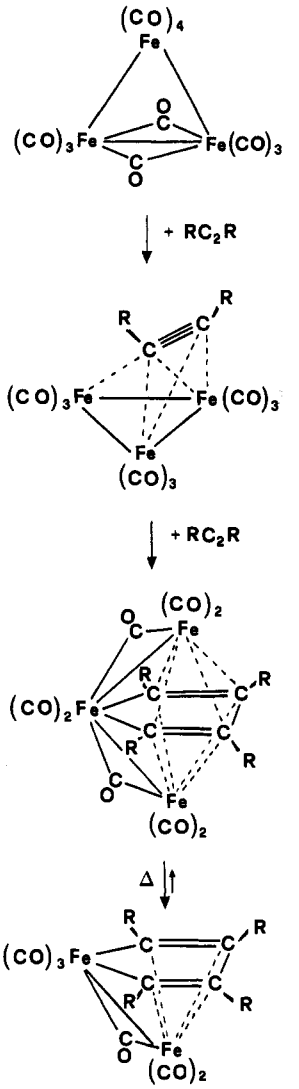

Figure 1. Sketch of the reaction sequence of $Fe_3(CO)_{12}$ with alkyne.

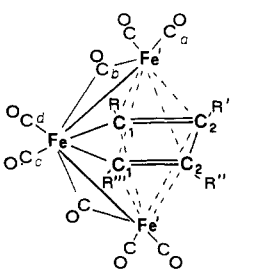

Figure 2. Structure of $Fe_3(CO)_8$(alkyne)$_2$ compounds.

Furthermore we have verified some detailed aspects of the reaction pathway by using mixed-metal (Fe, Ru) clusters.[22]

Optimization of this procedure has allowed us to obtain both the homosubstituted alkyne clusters of formula $Fe_3(CO)_8(RC_2R)_2$ (namely, **1**, R = Ph; **2**, R = Et) by simply refluxing $Fe_3(CO)_{12}$ with an excess of the appropriate alkyne in cyclohexane (yields: **1**, ca. 70%; **2**, ca. 60%) and heterosubstituted alkyne clusters of formula $Fe_3(CO)_8(RC_2R)(R'C_2R')$ (namely, **3**, R = Ph, R' = Et; **4**, R = Ph, R' = H; **5**, R = Et, R' = H) through two-step syntheses. The stable $Fe_3(CO)_9(RC_2R)$ intermediate is first obtained

(9) Casarin, M.; Ajò, D.; Granozzi, G.; Tondello, E.; Aime, S. *Inorg. Chem.* **1985**, *24*, 1241.
(10) Casarin, M.; Ajò, D.; Vittadini, A.; Ellis, D. E.; Granozzi, G.; Bertoncello, E.; Osella, D. *Inorg. Chem.* **1987**, *26*, 2041.
(11) For a recent discussion see: Mingos, D. M. P. *Acc. Chem. Res.* **1984**, *17*, 311 and references therein.
(12) Jaouen, G.; Marinetti, A.; Mentzen, B.; Mutin, R.; Saillard, J. Y.; Sayer, B. G.; McGlinchey, M. J. *Organometallics* **1982**, *1*, 753.
(13) Osella, D., unpublished work.
(14) (a) Kotz, J. C.; Petersen, J. V.; Reed, R. C. *J. Organomet. Chem.* **1976**, *120*, 433. (b) Peake, B. M.; Robinson, B. H.; Simpson, J.; Watson, D. J. *Inorg. Chem.* **1977**, *16*, 405.
(15) Zanello, P.; Aime, S.; Osella, D. *Organometallics* **1984**, *3*, 1374.
(16) Osella, D.; Gobetto, R.; Montangero, P.; Zanello, P.; Cinquantini, A. *Organometallics* **1986**, *5*, 1247.
(17) Osella, D.; Botta, M.; Gobetto, R.; Laschi, F.; Zanello, P. *Organometallics* **1988**, *7*, 283.
(18) Heinze, J. *Angew. Chem., Int. Ed. Engl.* **1984**, *23*, 831.
(19) Dessy, R. E.; Pohl, R. L. *J. Am. Chem. Soc.* **1968**, *90*, 1995.
(20) Blount, J. F.; Dahl, L. F.; Hoogzand, C.; Hubel, W. *J. Am. Chem. Soc.* **1966**, *88*, 292.
(21) Hock, A. A.; Mills, O. *Acta Crystallogr.* **1961**, *14*, 139.
(22) Busetti, V.; Granozzi, G.; Aime, S.; Gobetto, R.; Osella, D. *Organometallics* **1984**, *3*, 1510.

Table I. IR Data of Compounds 1–9

compounds	$\bar{\nu}_{CO}$, cm^{-1} (solvent *n*-hexane)						
$[Fe_3(CO)_8(PhC_2Ph)_2]$ (1)	2058 s	2020 s	2014 vs	2005 s	1975 s	1869 m	1856 m
$[Fe_3(CO)_8(EtC_2Et)_2]$ (2)	2053 s	2013 sh	2011 vs	1990 s	1970 s	1868 m	1856 m
$[Fe_3(CO)_8(PhC_2Ph)(EtC_2Et)]$ (3)	2057 s	2019 s	2013 vs	1999 s	1974 s	1868 m	1855 m
$[Fe_3(CO)_8(PhC_2Ph)(HC_2H)]$ (4)	2064 s	2026 s	2022 vs	2004 s	1983 s	1878 m	1866 m
$[Fe_3(CO)_8(EtC_2Et)(HC_2H)]$ (5)	2061 s	2023 s	2020 vs	1996 s	1980 s	1877 m	1867 m
$[Fe_3(CO)_8(MeC_2Ph)(HC_2H)]$ (6)	2062 s	2023 s	2021 vs	1998 s	1983 s	1876 m	1865 m
$[Fe_3(CO)_8(PhC_2Me)(HC_2H)]$ (7)	2063 s	2025 s	2021 vs	2001 s	1983 s	1877 m	1866 m
$[Fe_3(CO)_8(MeC_2Ph)(PhC_2Ph)]$ (8)	2058 s	2021 s	2014 vs	2005 s	1976 s	1870 m	1858 m
$[Fe_3(CO)_8(PhC_2Me)(PhC_2Ph)]$ (9)	2059 s	2021 s	2014 vs	2003 s	1975 s	1870 m	1858 m

Table II. ^{1}H NMR Data for Compounds 1–9 Recorded at 270.0 MHz

compounds	δ, ppm ($CDCl_3$)
$[Fe_3(CO)_8(PhC_2Ph)_2]$ (1)	7.45 (m, 4, *o*-PhC_2); 7.18 (m, 6, *m*+*p*-PhC_2); 6.83 (m, 6, *m*+*p*-PhC_1); 6.29 (m, 4, *o*-PhC_1)
$[Fe_3(CO)_8(EtC_2Et)_2]$ (2)	3.25 (q, 4, CH_2); 1.69 (t, 6, CH_3); 1.33 (q, 4, CH_2); 0.59 (t, 6, CH_3)
$[Fe_3(CO)_8(PhC_2Ph)EtC_2Et)]$ (3)	7.89 (m, 2, *o*-PhC_2); 7.47 (m, 3, *m*+*p*-PhC_2); 6.80 (m, 3, *m*+*p*-PhC_1); 6.19 (m, 2, *o*-PhC_1); 3.13 (q, 2, CH_2); 1.45 (t, 3, CH_3); 1.43 (q, 2, CH_2); 0.68 (t, 3, CH_3)
$[Fe_3(CO)_8(PhC_2Ph)(HC_2H)]$ (4)	7.80 (d, 1, J = 5.0 Hz); 7.64 (m, 2, *o*-PhC_2); 7.40 (m, 3, *m*+*p*-PhC_2); 6.92 (m, 3, *m*+*p*-PhC_1); 6.24 (m, 2, *o*-PhC_1); 2.37 (d, 1, J = 5.0 Hz)
$[Fe_3(CO)_8(EtC_2Et)(HC_2H)]$ (5)	7.60 (d, 1, J = 5.1 Hz); 3.11 (q, 2, CH_2); 2.23 (d, 1, J = 5.1 Hz); 2.0 (t, 3, CH_3); 1.22 (q, 2, CH_2); 0.48 (t, 3, CH_3)
$[Fe_3(CO)_8(MeC_2Ph)(HC_2H)]$ (6)	8.11 (m, 2, *o*-PhC_2); 7.72 (d, 1, J = 5.4 Hz); 7.61 (m, 3, *m*+*p*-PhC_2); 1.92 (d, 1, J = 5.4 Hz); 1.14 (s, 3, Me)
$[Fe_3(CO)_8(PhC_2Me)(HC_2H)]$ (7)	7.71 (d, 1, J = 5.0 Hz); 7.05 (3, m, *m*+*p*-PhC_1); 6.42 (m, 2, *o*-PhC_1); 2.94 (s, 3, CH_3); 2.49 (d, 1, J = 5.0 Hz)
$[Fe_3(CO)_8(MeC_2Ph)(PhC_2Ph)]$ (8)	7.85 (m, 4, *o*-PhC_2); 7.61 (m, 6, *m*+*p*-PhC_2); 6.85 (m, 3, *m*+*p*-PhC_1); 6.18 (m, 2, *o*-PhC_1); 1.16 (s, 3, CH_3)
$[Fe_3(CO)_8(PhC_2Me)(PhC_2Ph)]$ (9)	7.87 (m, 2, *o*-PhC_2); 7.60 (m, 3, *m*+*p*-PhC_2); 6.90 (m, 6, *m*+*p*-PhC_1); 6.15 (m, 4, *o*-PhC_1); 2.68 (s, 3, CH_3)

by heating $Fe_3(CO)_{12}$ with the appropriate alkyne (RC_2R) in *n*-hexane. It is then purified by TLC and reacted further with a different alkyne ($R'C_2R'$) in refluxing cyclohexane to give the desired $Fe_3(CO)_8(RC_2R)(R'C_2R')$ derivatives (yields 50–30%, depending on the nature of substituents).

Attempts to employ alkynes bearing substituents with pronounced electron-withdrawing or electron-releasing properties [e.g. $C_2(CF_3)_2$, $C_2(COOMe)_2$, or $C_2(CH_2NMe_2)_2$] were unsuccessful; extensive decomposition occurred and only binuclear $Fe_2(CO)_6(RC_2R)(R'C_2R')$ complexes could be isolated. Since theoretical calculations[9] suggest a delicate alkyne cluster charge balance, small perturbations may destabilize the entire molecule.

Figure 2 shows the structure of the synthesized compounds along with the numbering scheme used in the text. We have previously shown that the reaction of $Fe_3(CO)_{12}$ with 1-phenyl-2-propyne gives an inseparable (by column or TL chromatography) mixture of two isomers, namely, $Fe_3(CO)_9(MeC_2Ph)$ and $Fe_3(CO)_9(PhC_2Me)$, whose molecular ratio has been established to be 2:1.[23] This mixture reacts further under the above conditions with a different alkyne ($R'C_2R'$) to afford two isomers of formula $Fe_3(CO)_8$(1-phenyl-2-propyne)($R'C_2R'$) (**6**, **7**, R′ = H; **8**, **9**, R′ = Ph). Fortunately, these isomers are separable by TLC simply by employing extra-long silica-coated plates (80 cm). These isomers will prove useful in the NMR assignment (vide infra). The structural relationship between such isomers is depicted in Figure 3. The molecular ratio of starting material to products indicates that once the first molecule of alkyne is coordinated to the Fe_3 skeleton neither intramolecular rotation of the alkyne over the metallic triangle nor intermolecular exchange between

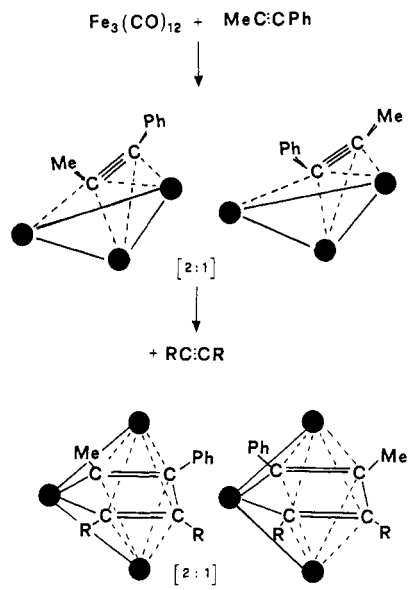

Figure 3. Structures of the two isomeric couples $Fe_3(CO)_9(C_2Me,Ph)$ and $Fe_3(CO)_8(C_2Me,Ph)(RC_2R)$ (R = H, **6** and **7**; R = Ph, **8** and **9**).

coordinated and free alkyne takes place up to the formation of the $Fe_3(CO)_8(alkyne)_2$ derivative.

The IR spectra of the synthesized compounds are reported in Table I; the strong similarity of their $\bar{\nu}$(CO) patterns suggests that their structures are identical in solution. Small differences can be ascribed to the different electronic effects of the alkyne substituents. It is worth noting that the number of resolved peaks does not increase on passing from homosubstituted to heterosubstituted alkyne compounds, in spite of the fact that in the latter the C_{2v} symmetry is completely lost. Apparently the substituents are not able to perturb the "$Fe_3(CO)_8C_4$" vibrational core.

All compounds exhibit the expected parent ion pattern in the electron-impact (EI) MS spectra.

(23) Granozzi, G.; Tondello, E.; Casarin, M.; Aime, S.; Osella, D. *Organometallics* **1983**, *2*, 430.
(24) Castiglioni, M.; Milone, L.; Osella, D.; Vaglio, G. A.; Valle, M. *Inorg. Chem.* **1976**, *15*, 394.
(25) Aime, S.; Milone, L.; Osella, D.; Valle, M. *J. Chem. Res., Synop.* **1978**, 77; *J. Chem. Res., Miniprint* **1978**, 782–790.

Table III. ^{13}C NMR Data for Compounds 1-9 Recorded at 67.9 MHz[a]

compounds	δ, ppm ($CDCl_3$)
$[Fe_3(CO)_8(PhC_2Ph)_2]$ (1)	203.0 (CO); 143.5-127.2 (Ph); 120.5, 119.0 (C_{ac})
$[Fe_3(CO)_8(EtC_2Et)_2]$ (2)	205.9 (CO); 128.1, 118.2 (C_{ac}); 33.6, 23.8 (CH_2); 20.2, 18.2 (CH_3)
$[Fe_2(CO)_8(PhC_2Ph)(EtC_2Et)]$ (3)	205.6, 202.9 (CO); 143.6, 126.6 (Ph); 128.2, 122.5, 121.7, 118.3 (C_{ac}); 33.9, 24.3 (CH_2); 19.5, 18.1 (CH_3)
$[Fe_3(CO)_8(PhC_2Ph)(HC_2H)]$ (4)	205.0, 202.7 (CO); 143.7-127.0 (Ph); 124.3, 120.5 (C_{ac}); 97.5, 93.1 (CH)
$[Fe_3(CO)_8(EtC_2Et)(HC_2H)$ (5)	205.8, 203.9 (CO); 127.8, 118.1 (C_{ac}); 98.6, 92.4 (CH); 33.1, 21.6 (CH_2); 17.8, 16.6 (CH_3)
$[Fe_3(CO)_8(MeC_2Ph)(HC_2H)]$ (6)	204.5, 203.7 (d, $^3J_{CH}$ = 3.0 Hz) (CO); 136.3, 122.7 (Ph); 119.6, 116.1 (C_{ac}); 97.9 (dd; $^1J_{CH}$ = 182.6 Hz; $^2J_{CH}$ = 1.4 Hz) (C_1-H); 92.3 (dd, $^1J_{CH}$ = 170.5 Hz; $^2J_{CH}$ = 1.7 Hz) (C_2-H); 28.4 (CH_3)
$[Fe_3(CO)_8(PhC_2Me)(HC_2H)]$ (7)	204.5, 203.5 (d, $^3J_{CH}$ = 3.0 Hz) (CO); 141.5-125.8 (Ph); 119.8, 111.6 (C_{ac}); 98.4 (dd; $^1J_{CH}$ = 170.1 Hz; $^2J_{CH}$ = 1.8 Hz) (C_1-H); 91.7 (dqd, $^1J_{CH}$ = 183.2 Hz; $^3J_{CH}$ = 3.6 Hz, $^2J_{CH}$ = 1.7 Hz) (C_2-H); 20.1 (CH_3)
$[Fe_3(CO)_8(MeC_2Ph)(PhC_2Ph)]$ (8)	204.5, 203.4 (CO); 144.1-121.9 (Ph); 120.7, 119.8, 119.0, 116.9 (C_{ac}); 28.7 (CH_3)
$[Fe_3(CO)_8(PhC_2Me)(PhC_2Ph)]$ (9)	203.8 (CO); 144.6-122.3 (Ph); 120.1, 119.3, 118.6, 111.5 (C_{ac}); 21.3 (CH_3)

[a] All proton-decoupled but those of 6 and 7.

Table IV. ^1H and ^{13}C NMR Chemical Shifts (δ, ppm) of $Fe_3(CO)_8(PhC_2Ph)_2$ (1) in CD_3COCD_3[a]

	^1H			^{13}C			
	o	m	p	C	o	m	p
Ph(C1)	6.50	7.07	7.12	143.8	129.5	127.3	127.6
Ph(C2)	7.74	7.43	7.36	133.9	133.4	129.2	128.0

[a] The choice of acetone-d_6 as solvent for the selective decoupling experiments comes from the better peak to peak separation achieved in this solvent with respect to $CDCl_3$, the solvent usually employed for the routine spectra reported in Tables II and III.

NMR Assignment. In the case of homosubstituted 1 and 2 as well as heterosubstituted alkyne clusters 3, 4, and 5 (both alkynes bearing identical substituents), no position isomerism is possible and the only question is the assignment of the substituent (Ph, Et, H) resonances.

The ^1H and ^{13}C NMR data are reported in Tables II and III, respectively. The large spread in the ^1H NMR chemical shift values of the substituents has no precedent in the binuclear homologues $M_2(CO)_6(RC_2R)_2$[26,27] (M = Fe, Ru, Os). This spread must be the consequence of the position of the substituents in the metallacycle; indeed the mixed-alkyne $Fe_3(CO)_8(PhC_2Ph)(EtC_2Et)$ derivative has a ^1H NMR spectrum that is almost superimposable on the spectra of $Fe_3(CO)_8(PhC_2Ph)_2$ (1) and $Fe_3(CO)_8(EtC_2Et)_2$ (2), each with half intensity. All the phenyl groups of the PhC=CPh moiety in 1, 3, 4, and 5 give rise to a similar pattern of complex multiplets of integrated intensity ratio 2:3:3:2 from low to high field. The ^1H NMR spectrum of 1 is shown in Figure 4.

From the ^1H COSY spectrum of 1 it is immediately apparent that the two downfield multiplets (2:3) and the two high-field ones (3:2) belong to the two different Ph groups. This is further confirmed by homonuclear decoupling experiments carried out on 1: upon irradiating each resonance of intensity 2 the corresponding resonance of intensity 3 becomes an AB_2 spin pattern. This indicates that the multiplets of intensity 2 correspond to the ortho protons and those of intensity 3 to the meta and para protons. Their chemical shifts are reported in Table IV.

The corresponding ^{13}C NMR spectra of 1 in the aromatic region is even more complex. However, selective heteronuclear decoupling experiments indicate unambiguously that the set of *downfield* multiplets in ^1H spectrum must be related to the set of *high-field* multiplets in ^{13}C spectrum and permit a complete assignment of the ^{13}C resonances (Table IV). It is commonly accepted[28] that the chemical shift difference between meta and para protons reflects the degree of conjugation of the phenyl ring; since this difference is quite small, no extensive conjugation between phenyl and π-electrons of the metallacycle should occur. This result is consistent with the finding that the phenyl rings do not lie in the same plane as the FeC_4 ring.[5]

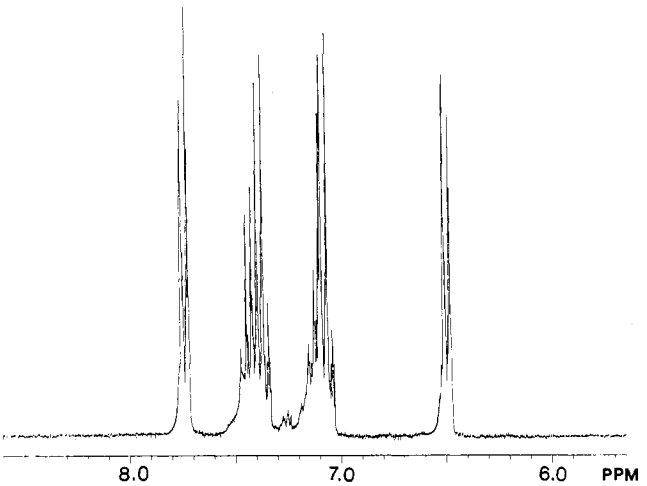

Figure 4. ^1H NMR spectrum of $Fe_3(CO)_8(PhC_2Ph)_2$ (1) recorded in CD_3COCD_3 solution at 270.0 MHz.

In spite of these results all resonances cannot be assigned absolutely. This can be done by NMR comparison of 6 and 7. The ^1H NMR spectrum of 6 exhibits in the phenyl region a pattern of multiplets in 2:3 integrated intensity ratio, while the spectrum of 7 shows a 3:2 pattern at a relatively higher field. Furthermore both isomers show a singlet for the methyl group and two doublets for the CH=CH moiety (see Table II). The ^{13}C NMR coupled spectrum of 6 shows, in the acetylenic region, two doublets of doublets, easily assigned to the CH=CH unit. No long-range coupling with the methyl protons can be observed for each signal. On the other hand, the spectrum of 7 shows two resonance in the same region. The *downfield* one is a doublet of doublets ($^1J_{CH}$ = 170.1 Hz, $^2J_{CH}$ = 1.8 Hz), while the *high-field* one can be interpreted as a doublet of quartets of doublets ($^1J_{CH}$ = 183.2 Hz, $^2J_{CH}$ = 1.7 Hz, $^3J_{CH}$ = 3.6 Hz) (Figure 5).

It follows that isomer 7 has the methyl substituent adjacent to the CH=CH moiety or, in other words, on the C_2 atom, and consequently isomer 6 has the methyl group on C_1. This assignment permits all the ^{13}C resonances of 6 and 7 and also all ^1H resonances, except those of the CH=CH moiety, to be assigned. In order to obtain this

(26) Aime, S.; Milone, L.; Sappa, E. *J. Chem. Soc., Dalton Trans.* **1976**, 838.
(27) Aime, S.; Occhiello, E. *J. Chem. Soc., Dalton Trans.* **1986**, 1863.
(28) Stothers, J. B. *C-13 NMR Spectroscopy*; Academic Press: New York, 1972.

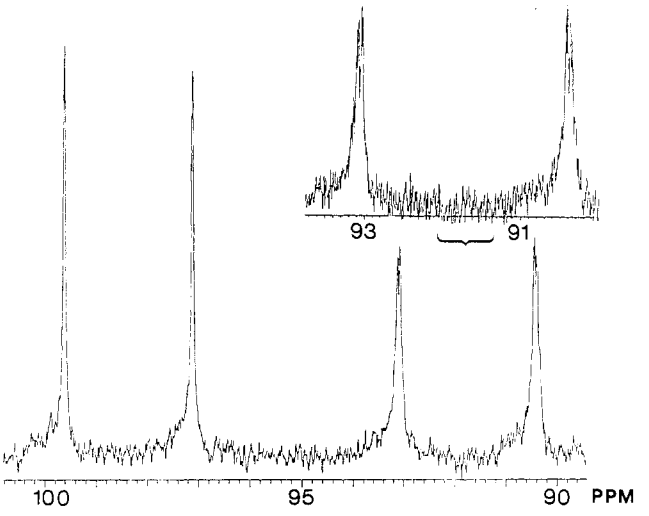

Figure 5. ^1H NMR spectrum of $Fe_3(CO)_8(PhC_2Me)(HC_2H)$ (7) in the acetylene region recorded in $CDCl_3$ solution at 270.0 MHz.

information, we have irradiated the *high-field* doublet (2.94 ppm) in the ^1H NMR spectrum of **6** and observed that the original *downfield* doublet (C_1–H) now appears as a singlet in the ^{13}C NMR spectrum. Therefore we can say that C_1 substituents resonate at a *higher* field with respect to C_2 ones in the ^1H NMR spectra. In contrast, C_1 substituents and C_1 atoms resonate at a *lower* field with respect to C_2 substituents and C_2 atoms in the ^{13}C NMR spectra.

The assignments in Tables II and III resulted from an extension of this concept to all derivatives under study. It is worth commenting that the trend in ^{13}C chemical shifts agrees with the generally accepted electron-withdrawing effect of the metal on σ/π-bonded carbon atoms[29] (C_1). The inverse trend in ^1H NMR spectra must be ascribed to the predominant anisotropic effect of nonbonding electrons of the transition metals. Comparison of the NMR spectra of $Fe_3(CO)_8(RC_2R)(HC_2H)$ (**4**–**7**) and $Fe_2(CO)_6(HC_2H)_2$[28] derivatives (where *both* ^{13}C and ^1H resonances at a lower field have been assigned to the C_1–H unit) indicates that the *formal* addition of the second apical Fe′ atom (Figure 1) renders the anisotropic effect predominant in the trinuclear compounds. Moreover the spread between C_1–H and C_2–H ^{13}C NMR resonances in the binuclear system spans 45 ppm,[27] in contrast to a range of only 5–6 ppm in trimetallic compounds. These data suggest an extensive electron delocalization within the metallacycle in the trimetallic systems.

Reinvestigation of the Dynamic Behavior. The room-temperature ^{13}C NMR spectra in the carbonyl region of the title complexes exhibit only resonances due to the CO's on the equatorial Fe atom; the remaining resonances are involved in a rapid localized exchange process.[6,7]

In the case of symmetrical derivatives (**1**, **2**) a single resonance is found for the two equivalent carbonyls of the $Fe(CO)_2$ moiety. The same situation holds for **9** (both CO's trans to CPh units). On the contrary the mixed-alkyne compounds **3**–**8** show two nearly coincident, but distinct, resonances. Moreover, for **4**–**7** the high-field peaks appear as doublets in the ^{13}C NMR proton-coupled spectra due to their trans relationship with a CH unit of the metallacycle. This differentiation prompted us to carry out a variable-temperature (VT) ^{13}C NMR study on the model

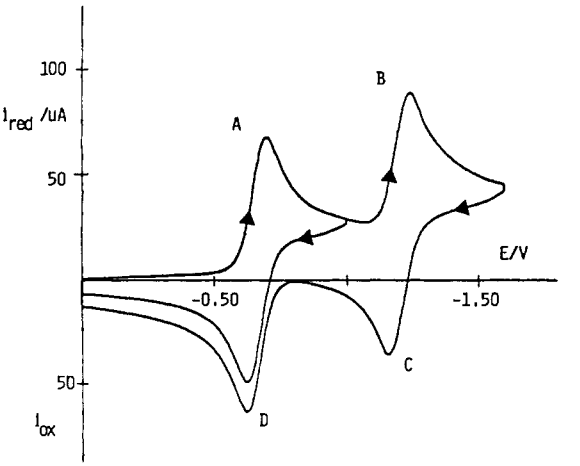

Figure 6. Cyclic voltammogram recorded at a mercury electrode on a MeCN solution containing **1** (2.0×10^{-3} mol dm^{-3}) and $[NEt_4]ClO_4$ (0.1 mol dm^{-3}). Scan rate = 0.2 V s^{-1}.

complex $Fe_3(CO)_8(EtC_2Et)(HC_2H)$ (**5**) synthesized by using a sample of $Fe_3(CO)_{12}$ ca. 40% ^{13}CO enriched. At −60 °C four resonances are observed at 253.6 (s), 205.4 (s), 204.9 (s), and 203.2 ppm (d, $^3J_{CH}$ = 3.0 Hz) in the integrated intensity ratio of 2:4:1:1, which can be easily assigned to CO_b, CO_a, CO_c, and CO_d, respectively (see Figure 2). When the temperature is raised the two downfield peaks broaden, collapse into the base line at ambient temperature, and eventually merge into a single peak at a higher temperature.[6,7] Interestingly, the two upfield resonances remain unchanged up to the decomposition temperature, indicating that the equatorial $Fe(CO)_2$ moiety as well as the FeC_4R_4 ring is static, as expected for a closo pentagonal-bipyramidal assembly, where the absence of any vacant site prevents fluxional processes involving the entire cluster. The sample is enriched enough so that $^2J_{CC}$ between CO_c and CO_d (ca. 7.0 Hz) can be observed. This value is in the range found for the cis CO–CO coupling constant in metal carbonyl clusters.[31]

Finally, the ^{13}C NMR proton-coupled spectrum in the acetylenic region exhibits two resonances at 98.6 (C_1H) and 92.4 (C_2H) ppm (Table III). Interestingly the *downfield* signal is now an apparent triplet due to the superposition of a singlet [isotopomer (60%) with CH trans to ^{12}CO] and a doublet [isotopomer (40%) with CH trans to ^{13}CO, $^2J_{CC}$ ca. 2 Hz]. This coupling pattern confirms its previous assignment to the C_1–H unit.

Electrochemical Behavior of Derivatives 1–9. In Figure 6 the cathodic part of the cyclic voltammogram (CV) displayed by $Fe_3(CO)_8(PhC_2Ph)_2$ (**1**) in acetonitrile is reported. Two distinct, well-shaped reduction waves are observed (peak A at E_p = −0.70 V and B at E_p = −1.24 V), each coupled with oxidation waves C and D in the reverse scan. Controlled potential coulometric tests carried out at a mercury pool working macroelectrode indicate that the first cathodic process (E_w = −0.85 V) consumes 1 mol of electrons/mol of **1**. Analysis of waves A and D at scan rates varying from 0.020 to 50 V s^{-1} indicates the following: the anodic to cathodic peak current ratio, $i_p(D)/i_p(A)$, is almost always equal to unity; the ratio between the cathodic peak current and the square root of the scan rate, $i_p(A)/v^{1/2}$, remains nearly constant; the difference between the potential of the cathodic peak and that of its directly associated reoxidation peak, $E_p(D) - E_p(A) = \Delta E_p$, gradually increases from 68 to 120 mV. Uncompensated resistance in solution is not significantly responsible for this

(29) Nesmeyanov, A. N.; Rybinskaya, M. I.; Rybin, L. V.; Kaganovich, V. S.; Petrovskii, P. V. *J. Organomet. Chem.* **1971**, *31*, 257.
(30) Halet, J. F.; Jaouen, G.; McGlinchey, M.; Jaillard, J. Y. *L'Actualité Chimique* **1985**, Avril, 23.
(31) Aime, S.; Osella, D. *J. Chem. Soc., Chem. Commun.* **1981**, 300.

Table V. Redox Potentials (in V vs SCE) for the Electron-Transfer Processes of Compounds 1–9 in MeCN or CH_2Cl_2 Solutions Containing $[NEt_4][ClO_4]$ (0.1 mol dm^{-3}) Supporting Electrolyte

	0/1−				0/1+		1/2+	
	$E^{\circ\prime}$, V		$E^{\circ\prime}$, V		$E^{a,a}$ V		$E^{a,a}$ V	
compounds	MeCN	CH_2Cl_2	MeCN	CH_2Cl_2	MeCN	CH_2Cl_2	MeCN	CH_2Cl_2
$[Fe_3(CO)_8(PhC_2Ph)_2]$ (1)	−0.66	−0.75	−1.20	−1.31	+1.21	+1.31	+1.36	+1.45
$[Fe_3(CO)_8(EtC_2Et)_2]$ (2)	−0.81	−0.94	−1.45	−1.61	+1.21	+0.97	+1.08	+1.43
$[Fe_3(CO)_8(PhC_2Ph)(EtC_2Et)]$ (3)	−0.76	−0.83	−1.38	−1.44	+0.98	+1.21	+1.12	+1.38
$[Fe_3(CO)_8(PhC_2Ph)(HC_2H)]$ (4)	−0.70	−0.74	−1.28	−1.33	+0.94	+1.13	+1.13	+1.42
$[Fe_3(CO)_8(EtC_2Et)(HC_2H)]$ (5)	−0.81	−0.86	−1.45	−1.54	+0.99	+1.15	+1.17	+1.56
$[Fe_3(CO)_8(MeC_2Ph)nHC_2H)]$ (6)	−0.74	−0.83	−1.33	−1.49	+1.06	+1.23	+1.23	+1.56
$[Fe_3(CO)_8(PhC_2Me)(HC_2H)]$ (7)	−0.73	−0.79	−1.32	−1.41	+1.05	+1.08	+1.26	+1.28
$[Fe_3(CO)_8(MeC_2Ph)(PhC_2Ph)]$ (8)	−0.73	−0.80	−1.29	−1.35	+1.18	+1.27	+1.30	+1.39
$[Fe_3(CO)_8(PhC_2Me)(PhC_2Ph)]$ (9)	−0.72	−0.78	−1.28	−1.33	+1.20	+1.28	+1.32	+1.40

[a] Peak potential values at 0.2 V s^{-1} for irreversible processes.

Table VI. Pseudopotential ab Initio Results for the Model Complex $Fe_3(CO)_8(HC_2H)_2$[a] (C_{2v} Symmetry)

	eigen-	population, %							
MO	value, eV	Fe	2Fe′	$2C_1$	$2C_2$	4H	$2CO_{sb}$	$6CO_t$	dominant character
$16b_2$ (LUMO)[c]	−0.48	14	15	25	4	0	28	14	Fe–Fe′ antibonding, with strong admixture of π^*_3 C_4H_4–MO
$22a_1$ (HOMO)[b]	−7.73	21	8	0	0	0	56	15	Fe–CO_{sb} back-bonding [Fe→(CO_{sb})]
$15b_2$[b]	−8.93	7	25	24	10	0	27	7	Fe′–C_4H_4 bonding [Fe′→π^*_3]

[a] See Figure 3 for atom numbering. Abbreviations: sb, semibridging; t, terminal. [b] Reference 9. [c] Granozzi, G.; Casarin, M., personal communication.

ΔE_p since the peak separation of ferrocene/ferrocenium couple ranges between 65 and 80 mV under identical conditions.

All these data are diagnostic[32] for an one-electron (1 → 1^-) *quasi-reversible* charge transfer, *uncomplicated* by following chemical reactions, occurring at the formal electrode potential $E^{\circ\prime}(0/1-) \cong E_{1/2} = [E_p(A) + E_p(D)]/2 = -0.66$ V. Besides the CV and coulometric data, evidence of a quasi-reversible one-electron process associated with A/D system comes from rotating disk electrode (RDE) technique at a Pt electrode: the slope of the plot of E vs log $[(i_l - i)/i]$ is 60 mV.

The same is true as far as the second redox process (B/C) is concerned; $E^{\circ\prime}(1-/2-) = -1.20$ V. However, in spite of the fact that the $i_p(C)/i_p(B)$ ratio is equal to unity even at the slowest scan rate (20 mV s^{-1}), which suggests a *chemically reversible* electron transfer, during controlled potential coulometric tests ($E_w = -1.40$ V) up to 5 electrons/molecule of 1 are consumed. The electrogenerated dianion must undergo a slow chemical reaction which generates secondary products that are electroactive at the working electrode potential. The half-life of the electrogenerated dianion $(1)^{2-}$ must be some tens of seconds.[33] This voltammetric scenario is common to all the triiron derivatives **1–9**, both in a coordinating solvent such as acetonitrile as well as in a noncoordinating solvent such as dichloromethane. The relevant redox potentials are reported in Table V. Interestingly, at a platinum electrode the second electron transfer (1−/2−) is considerably less reversible, $E_p(C) - E_p(B)$ being 120 mV, even at the slowest scan rate (20 mV s^{-1}). The difference between the formal electrode potentials in the two subsequent cathodic reductions, $\Delta E^{\circ\prime} = E^{\circ\prime}(0/1-) - E^{\circ\prime}(1-/2-)$, is of the order of 600 mV, regardless of the substituents in the metallacycle, the solvent, and the electrode material. It is well established that the difference in energy between two subsequent additions of electrons into a molecule is a measure of the Coulombic effect of the added charges and the delocalization and/or reorganization energy.[34]

The constant difference $\Delta E^{\circ\prime}$ in all the isoelectronic and isostructural derivatives **1–9** suggests that both electrons are added to a nondegenerate LUMO (the dianion is ESR silent, vide infra), a situation similar to that found for aromatic hydrocarbons.[35] This difference can be assumed to represent, to a first approximation, the energy required to overcome electronic repulsion within the same molecular orbital (ca. 58 kJ mol^{-1}). A similar value has been found for homo- and hetero metallic C-, Ge-, or P-capped trinuclear clusters.[36]

This remarkable difference of the two, subsequent, reduction potentials also indicates a strong instability of the electrogenerated dianions toward the conproportionation reaction:

$$(1) + (1)^{2-} \xrightarrow{K_{con}} 2(1)^-$$

The value of K_{con} can be obtained[18] from the known potentials $E^{\circ\prime}(0/1-)$ and $E^{\circ\prime}(1-/2-)$. In the present case an average value of 1.4×10^{10} can be evaluated for the triiron derivatives under study.

Moreover, the constant $\Delta E^{\circ\prime}$ suggests that no substantial structural changes take place in the $Fe_3(CO)_8(alkyne)_2$ clusters during the reduction. Occasionally, a geometric reorganization can facilitate the second reduction step by making $E^{\circ\prime}(1-/2-)$ less negative than that expected simply on the basis of electrostatic effects. This is the case for $Fe_3(CO)_9(alkyne)$ clusters.[16] The two subsequent reversible cathodic reductions have a $\Delta E^{\circ\prime}$ of about 200 mV, while concomitant with the reduction the orientation of the alkyne moiety relative to the metallic triangle is changed from perpendicular to parallel.

The redox potential of clusters **1–9** are quite sensitive to the electronic nature of the R in the metallacyclopentadienyl ring. As expected, electron-donating groups

(32) (a) Sauthampton Electrochemistry Group In *Instrumental Methods in Electrochemistry*; Wiley: Chichester, 1985. (b) Brown, E. R.; Sandifer, J. R. In *Physical Methods of Chemistry Electrochemical Methods*; Rossiter, B. W., Hamilton, J. F., Eds.; Wiley: New York, 1986; Vol. 2, Chapter 4.

(33) Adams, R. N. In *Electrochemistry at Solid Electrodes*, Marcel Dekker: New York, 1969.

(34) Gagné, R. R.; Koval, C. A.; Smith, T. J.; Cimolino, M. C. *J. Am. Chem. Soc.* **1979**, *101*, 4571.

(35) McKinney, T. M. *Electroanal. Chem.* **1980**, *10*, 97.

(36) Lindsay, P. N.; Peaks, B. M.; Robinson, B. N.; Simpson, J.; Honrath, U.; Vahrenkamp, H. *Organometallics* **1984**, *3*, 413.

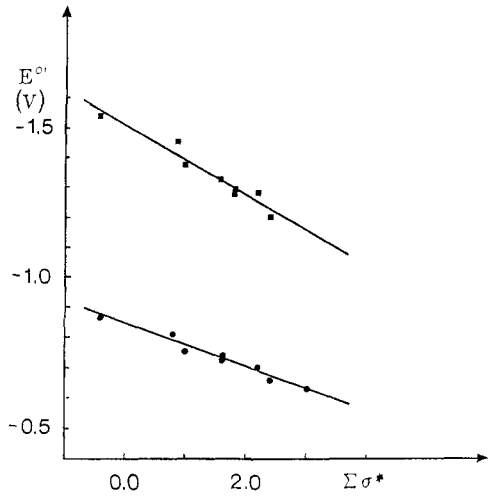

Figure 7. Plot of $E^{\circ\prime}$ for reduction (●, 0/1−; ■, 1−/2−) of $Fe_3(CO)_8(alkyne)_2$ compounds against the sum of the Taft's σ^* values of the substituents. The least-squares slopes are 0.071 V (●) and 0.118 V (■), respectively, and the correlation coefficients are 0.981 (●) and 0.979 (■), respectively.

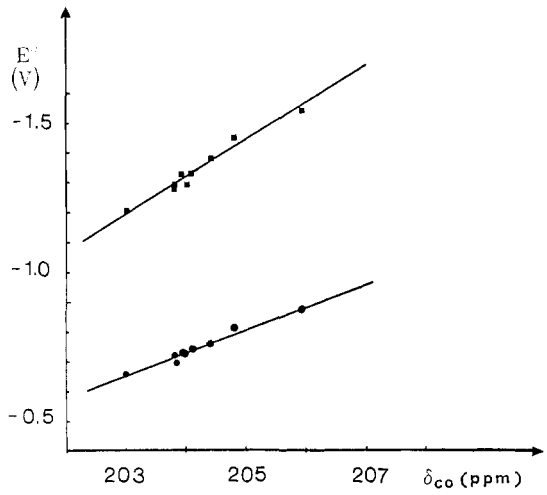

Figure 8. Plot of $E^{\circ\prime}$ for reduction (●, 0/1−; ■, 1−/2−) of $Fe_3(CO)_8(alkyne)_2$ compounds against $\delta(^{13}C)$ average of CO groups of the $Fe(CO)_2$ moiety. The least-squares slopes are −0.076 (●) and −0.125 V/ppm (■), respectively, and the correlation coefficients are 0.989 (●) and 0.983 (■), respectively.

disfavor the reduction processes, whereas electron-withdrawing ones facilitate them. In more quantitative terms, the formal electrode potentials $E^{\circ\prime}$ are proportional to the field effect of the R substituents (evaluated through their Taft's σ^* values).[37] Excellent linear correlations can be obtained by plotting the sums of the Taft's σ^* values of the substituents (regardless of their position in the metallacycle) against the $E^{\circ\prime}$ values (Figure 7). This correlation suggests a high electronic delocalization in the whole cluster in agreement with the previous theoretical study.[9] In particular, the LUMO ($16b_2$) is metal–metal antibonding in character with strong admixture of the π^*_3 MO of the "biradical" butadiene fragment (Table VI). This is responsible for the efficient electron delocalization and for the stability of the electrogenerated anions.

(37) (a) Taft, R. W., Jr. In *Steric Effects in Organic Chemistry*; Newman, M. S., Ed.; Wiley: New York, 1956. (b) σ^* is by no means a measure of inductive effects, but it also contains a resonance component; see for example: Martin, Y. C. In *Quantitative Drug Design*; Marcel Dekker: New York, 1972. March, J. In *Advances Organic Chemistry*; McGraw-Hill: Tokyo, 1980.

(38) Bond, A. M.; Carr, S. W.; Colton, R.; Kelly, D. P. *Inorg. Chem.* 1983, *22*, 989.

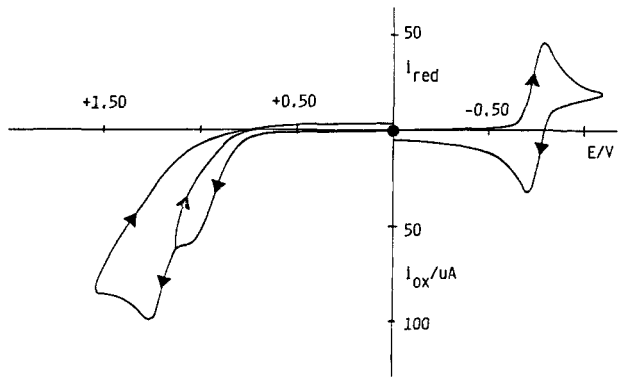

Figure 9. Cyclic voltammetric response recorded at a platinum electrode in a MeCN solution containing $Fe_3(CO)_8(MeC_2Ph)(HC_2H)$ (**6**) (2.4×10^{-3} mol dm^{-3}) and $[NEt_4]ClO_4$ (0.1 mol dm^{-3}) [scan rate = 0.2 V s^{-1}; (●) starting potential).

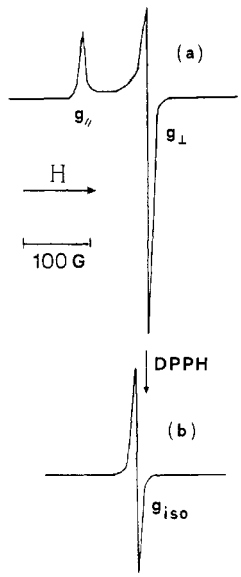

Figure 10. X-Band ESR spectrum of $[1]^-$, electrogenerated in MeCN solution ($[NEt_4]ClO_4$ = 0.1 mol dm^{-3}): trace a, 100 K; trace b, 292 K.

In striking contrast, different organometallic complexes such as flyover bridge derivatives, $[Fe_2(CO)_6(RC_2R)_2CO]$, where localized FeC σ bonds have been suggested, show a linear correlation between $E^{\circ\prime}$ and values of *only* the substituents on the carbon atoms adjacent to the metallic framework.[17]

Moreover, linear correlations (Figure 8) are found between the $E^{\circ\prime}$ values of each reduction step and the average $\delta(^{13}CO)$ values of the carbonyl groups of the $Fe(CO)_2$ moiety, the only ones detectable at room temperature for compounds **1**–**9** (vide supra). This free energy correlation has been already discussed by Bond and co-workers[28] and verified by us for a number of organometallic clusters.[15-17]

Finally, the ferracyclopentadienyl complexes **1**–**9** also undergo two successive, closely spaced, oxidation processes at a platinum electrode. In Figure 9 the cyclic voltammogram of **6** is reported as an example; the relevant values are listed in Table V. The two anodic peaks do not correlate with reduction responses in reverse scans even at scan rate as high as 50 V s^{-1}. Comparison of peak heights with that of the fully reversible 0/1− redox change allows us to interpret at least the first wave as the 0/1+ electron-transfer process. The proximity of the waves to the solvent discharge and their poor reproducibility discouraged us from a more thorough investigation. It is likely that the lack of reduction waves in reverse scans is due to

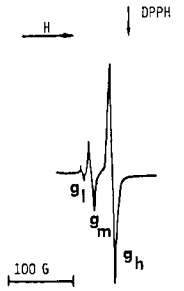

Figure 11. Room-temperature X-band ESR spectrum of the species resulting from macroelectrolysis of 1 after the consumption of 2 faradays/mol at −1.40 V (MeCN solution; $[NEt_4]ClO_4$ = 0.1 mol dm^{-3}).

a fast coupled chemical reaction (EC mechanism) rather than to an intrinsic slowness of the heterogeneous electron transfer (i.e. electrochemical *irreversibility*), as previously found for other alkyne clusters.[15-17] Loss of electrons from the HOMO ($22a_1$, Table VI) of these systems[9] should destabilize the entire molecule.

Mechanistic Proposal. During the bulk electrolysis of 1 (E_w = −0.85 V), the acetonitrile solution turns from black-green to deep brown. The resulting electrogenerated monoanion $(1)^-$ has been examined by electron spin resonance (ESR) spectroscopy. In Figure 10 the X-band spectra, both a liquid-nitrogen temperature (100 K, trace a) and at room temperature (298 K, trace b), are shown. The frozen solution spectrum is characterized by a well-resolved axial structure ($g_\parallel$ = 2.061; $g_\perp$ = 2.000) that suggests an iron-centered radical. At room temperature with signal becomes isotropic (g_{iso} = 2.020, ΔH_{iso} = 5.9 G), in agreement with Dessy's result.[19] The small difference in the g value can be ascribed to the different solvent employed. The 0/1− reduction is completely chemically reversible: reoxidation of the solution at 0.00 V or by air (O_2) or excess of $AgPF_6$ regenerates the starting species 1.

As far as the $(1)^- \rightarrow (1)^{2-}$ redox change is concerned, a number of experimental data have to be taken into account. As previously stated, the controlled potential coulometry indicates that the dianion is quite unstable. Exhaustive electrolyses performed at E_w = −1.40 V, corresponding to the consumption of 2, 3, 4, or 5 electrons/molecule, followed by chemical reoxidation by air and TLC separation, afforded decreasing amounts of the neutral parent cluster 1, along with increasing amounts of both the homologous binuclear $Fe_2(CO)_6(PhC_2Ph)_2$ complex[2] (easily identified by IR and MS spectrometry) and an intractable brown residue (which does not exhibit any absorption in the IR $\bar{\nu}$(CO) region).

The room-temperature X-band ESR spectrum of the deep red acetonitrile solution resulting from 2 faradays/mol reduction of 1 is reported in Figure 11. Three paramagnetic species are present in the electrolyzed solution: g_h = 2.020 and ΔH_h = 6.0 G [clearly due to the monoanion (1^-)], g_m = 2.039 and ΔH_m = 5.1 G, and g_1 = 2.049 and ΔH_1 = 4.8 G. We can assign the last two resonances to different iron-centered radicals,[39] in view of the large magnitude of the g value as well as the corresponding peak-to-peak separation (ΔH).

Qualitatively similar ESR responses have been obtained at room temperature from 3, 4, 5 or electrons/molecule

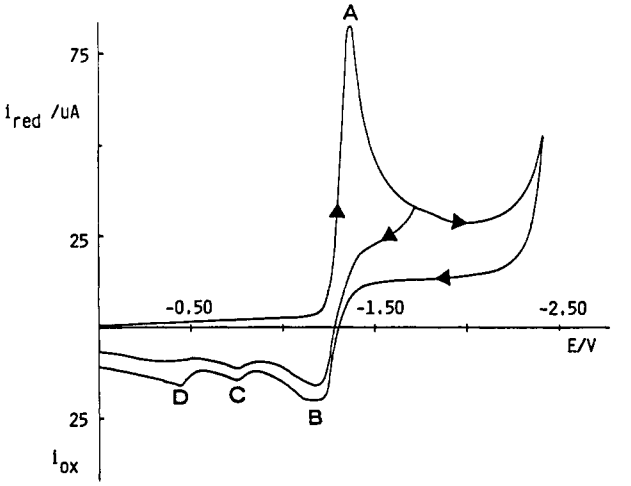

Figure 12. Cyclic voltammogram recorded at a mercury electrode on a MeCN solution containing $Fe_2(CO)_6(PhC_2Ph)_2$ (1.2×10^{-3} mol dm^{-3}) and $[NEt_4]ClO_4$ (0.1 mol dm^{-3}). Scan rate = 0.2 V s^{-1}.

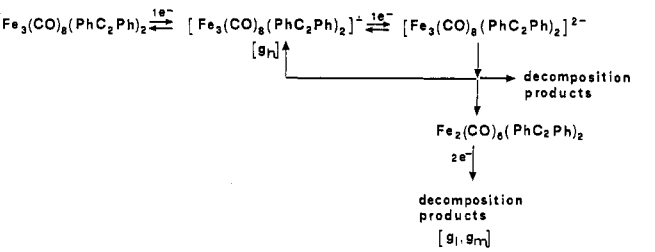

Figure 13. Scheme of the electrochemical events undergone by $Fe_3(CO)_8(PhC_2Ph)_2$ (1) both in CV and electrolysis experiments.

electrolyzed solutions, the only difference being a minor abundance of the monoanion with respect to the species responsible for signals at g_1 and g_m.

Since the $Fe_2(CO)_6(PhC_2Ph)_2$ complex has been recovered after the reduction/chemical reoxidation cycle (vide supra), we have undertaken a CV investigation on the redox behavior of this derivative (only brief reports of similar ferrole compounds have been published so far[19,40]). Figure 12 shows the CV response of $Fe_2(CO)_6(PhC_2Ph)_2$ in acetonitrile solution. A reduction wave (A) (E_p = −1.36 V) is associated with an oxidation wave (B) in the reverse scan. However, the fact that the $i_p(B)/i_p(A)$ ratio is less than unity (0.8), even at scan rate as high as 10 V s^{-1}, and the presence of other anodic peaks (C, D) suggests that a fast chemical reaction follows the reduction process. Controlled potential coulometry at E_w = −1.40 V shows that 2 electrons/molecule are consumed quickly and a third more slowly.

The ambient-temperature ESR spectrum of the red solution that results from electrolysis of $Fe_2(CO)_6(PhC_2Ph)_2$ exhibits two lines centered at almost the same g values (namely, 2.039 and 2.048) as those found in the electrolysis of $Fe_3(CO)_8(PhC_2Ph)_2$. On the basis of these data we can propose a mechanism for the overall reduction processes $(1) \rightarrow (1)^- \rightarrow (1)^{2-}$, even if the full stoichiometric balance is prevented by the formation of unidentified decomposition products. As previously stated, in the CV time scale both $(1) \rightarrow (1)^-$ and $(1)^- \rightarrow (1)^{2-}$ processes are *chemically* reversible. During longer electrolyses the dianion smoothly disproportionates to monoanion, to the dinuclear $Fe_2(CO)_6(PhC_2Ph)_2$ complex, and probably to other unidentifiable compounds. The binuclear complex

(39) (a) Muetterties, E. L.; Sosinsky, B. A.; Zamaraev, K. I. *J. Am. Chem. Soc.* **1975**, *97*, 5299. (b) Krusic, P. J.; Filippo, J. S., Jr.; Hutchinson, B.; Hance, R. L.; Daniels, L. M. *J. Am. Chem. Soc.* **1981**, *103*, 2129. (c) Collman, J. P.; Finke, R. G.; Mathock, P. L.; Wahren, R.; Komoto, R. G.; Brauman, J. I. *J. Am. Chem. Soc.* **1978**, *100*, 1119. (d) Krusic, P. J.; Cote, W. J.; Grand, A. *J. Am. Chem. Soc.* **1984**, *106*, 4642.

(40) Zotti, G.; Rieke, R. D.; McKennis, J. S. *J. Organomet. Chem.* **1982**, *228*, 281.

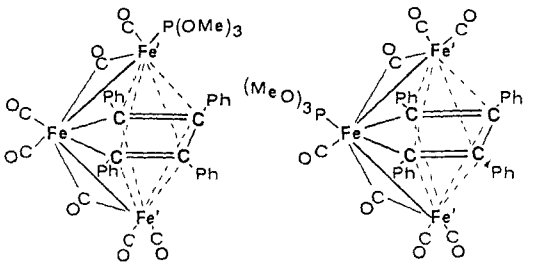

Figure 14. Structures of $[Fe_3(CO)_7P(OMe)_3(PhC_2Ph)_2]$ isomers **10** and **11**.

is, in turn, electroactive at the working potential (E_w = −1.40 V) and produces two paramagnetic species responsible for the ESR resonances at g_1 and g_m values. Unfortunately, these species do not afford, after chemical reoxidation, any isolable compounds. The formation of $[Fe_3(CO)_8(PhC_2Ph)_2]^-$ and $Fe_2(CO)_6(PhC_2Ph)_2$ explains the large number of electrons (up to 5) spent in the exhaustive electrolysis of $Fe_3(CO)_8(PhC_2Ph)_2$ at the second reduction step. From the bulk of ESR data we must conclude that the unstable dianion $(1)^{2-}$ is ESR silent or, in other words, is a diamagnetic species (singlet spin state). This agrees with the previous proposal, forwarded on the basis of the constant $\Delta E^{\circ\prime}$ value, the the added electrons enter a nondegenerate LUMO ($16b_2$ in Table VI) and make the cluster susceptible to Fe–Fe′ bond rupture.

Electron-Transfer Chain (ETC) Synthesis of $[Fe_3(CO)_7P(OMe)_3(PhC_2Ph)_2]$ (10, 11) Isomers. Electron-transfer chain catalysis is a general class of reactions in which electron-transfer steps are employed in order to accelerate transformations that otherwise are too slow.[41] Electron-induced nucleophilic substitutions have been extensively applied to organometallic systems.[42] The key feature is the preparation by electrolysis of long-lived radical anions, which can rapidly undergo nucleophilic substitution of Lewis bases for CO and then transfer the extra electron to unreduced substrate (ĒCĒ mechanism). With the aim of applying such ETC reaction to the title ferracyclopentadienyl clusters, we have investigated the CV behavior of **10** and **11** easily obtained through the $[Fe(CO)_2Cp]_2$-catalyzed synthesis;[43] their structures are depicted in Figure 14. Both isomers give rise to two distinct, well-behaved reduction waves in the cathodic CV response at $E^{\circ\prime}$ (0/1−) = −0.98 V and $E^{\circ\prime}$(1−/2−) = −1.24 V for **10** and at $E^{\circ\prime}$(0/1−) = −1.03 V and $E^{\circ\prime}$(1−/2−) = −1.24 V for **11**, respectively (CH_2Cl_2/$(Bu_4N)ClO_4$ solution, Hg electrode). The CV features of the most abundant, dark green isomer **10** are reported in Figure 15. Analysis of the first cathodic CV response at scan rates varying from 0.020 to 10 V s^{-1} shows that it involves a chemical complication following the reduction (EC mechanism). An half-life of about 5 s can be computed for $(10)^-$.[33]

ESR investigation on the solution obtained by macroelectrolysis at E_w = −1.05 V confirms this behavior. The room-temperature ESR spectrum recorded at the first stages of the electrolysis (0.2 faraday/mol of **10**) shows a pattern similar to that of $(1)^-$ (g_{iso} = 2.021), whereas at longer times (0.6 faraday/mol of **10**) new resonances accompany this most abundant absorption. We have not

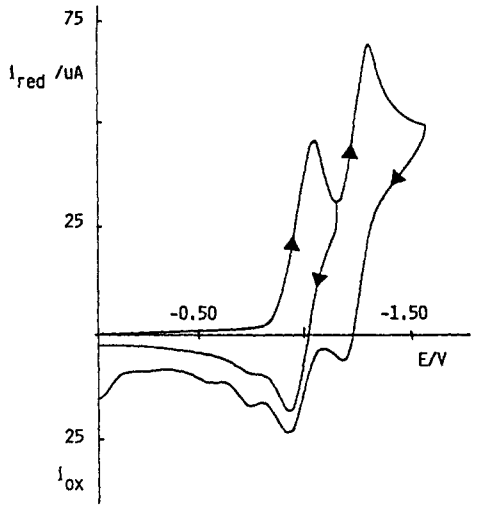

Figure 15. Cyclic voltammogram recorded at a mercury electrode on a CH_2Cl_2 solution containing **10** (1.2×10^{-3} mol dm^{-3}) and $[NBu_4]ClO_4$ (0.1 mol dm^{-3}). Scan rate = 0.2 V s^{-1}.

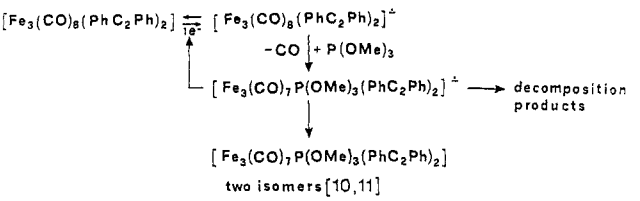

Figure 16. Scheme of the ETC process.

investigated the nature of these decomposition products further. The same features hold for **11**.

The existence of a (0/1−) process for both isomers **10** and **11** at potentials well more negative than that for the parent cluster $Fe_3(CO)_8(PhC_2Ph)_2$ (as expected on the basis of the better σ donor/π acceptor ratio of $P(OMe)_3$ with respect to CO ligand) indicates that the ĒCĒ mechanism can, in principle, take place. Indeed, electrolysis of **1** at the mercury pool electrode (E_w = −0.85 V; 0.2 faraday/mol) in the presence of a slight excess of $P(OMe)_3$ rapidly converts **1** to both **10** and **11** isomers, as verified by CV experiments and by chemical reoxidation of the mixture by air (O_2) and subsequent TLC workup (yields: **10**, ca. 50%; **11**, ca. 25%). The ETC reaction is depicted in Figure 16. Since the substituted monoanions $(10)^-$ and $(11)^-$ are quite unstable, the efficiency of the ETC mechanism (as indicated from the reasonable yield obtained) confirms that the transfer of the extra electron from $(10)^-$ and $(11)^-$ to $(1)^-$ occurs very rapidly, well before extensive decomposition. This ETC reaction is not regioselective[44] as expected by the closeness of the $E^{\circ\prime}$(0/1−) values of **10** and **11**. In fact **10** and **11** were obtained in a molecular ratio of ca. 2:1, which corresponds to the statistical Fe and Fe′ ratio. This indicates that the increased electron density caused by the $P(OMe)_3$ ligand on the Fe′ atom in **10** and on the Fe atom in **11** is efficiently redistributed over the whole cluster in agreement with the similar g_{iso} values of $(1)^-$, $(10)^-$, and $(11)^-$.

Experimental Section

The $Fe_3(CO)_8(alkyne)_2$ compounds were prepared by slight modification of the literature procedure[2] as briefly described in the Results and Discussion. The IR and mass spectra were recorded on a Perkin-Elmer 580B and on AEI MS12 instruments, respectively. The ^1H and ^{13}C NMR spectra were recorded on a

(41) Chanon, M.; Tobe, M. L. *Angew. Chem., Int. Ed. Engl.* **1982**, *21*, 1.

(42) Kochi, J. K. *J. Organomet. Chem.* **1986**, *300*, 139 and references therein.

(43) Aime, S.; Botta, M.; Gobetto, R.; Osella, D. *Inorg. Chem. Acta* **1986**, *115*, 129.

(44) Arewgoda, C. M.; Robinson, B. H.; Simpson, J. *J. Chem. Soc., Chem. Commun.* **1982**, 284.

JEOL GX-270-89 spectrometer. The EPR spectra were obtained from a Bruker 200 D-SRC instrument operating at 9.78 GHz (X-band) equipped with a Bruker variable-temperature ER 411 VT unit. The electrochemical apparatus and the purifications of solvents and supporting electrolytes have been described previously.[15-17] All potentials are referred to the saturated calomel electrode (SCE). Under the actual experimental conditions the ferrocene/ferrocenium couple is located at +0.38 V in MeCN and +0.49 V in CH_2Cl_2. Separation workup was brought about by SiO_2 column chromatography [eluent petroleum ether (40–70 °C) with increasing amount of CH_2Cl_2]. The identification of $Fe_2(CO)_6(PhC_2Ph)_2$ was achieved by IR and MS spectrometry and TLC comparison with autentical sample.

Acknowledgment. We thank the Ministry of Public Education (M.P.I., Rome), the Council of National Research (CNR, Rome), and the European Economic Community (EEC) for financial support and Prof. G. Granozzi and M. Casarin (University of Padua) for the extension of the ab initio calculations to the LUMO of the model complex $Fe_3(CO)_8(HC_2H)_2$.

Reactions of Disubstituted Alkynes with Bromotris(trimethylphosphine)cobalt(I). Synthesis and Molecular and Crystal Structures of $[Co(\eta^2\text{-}PhC{\equiv}CC_5H_{11})(PMe_3)_3]BPh_4$ and $[Co(\sigma^2\text{-}(CO_2Me)_4C_4)(MeCN)_2(PMe_3)_2]BPh_4$

Abdessalam Bouayad, Michèle Dartiguenave,* Marie-Joëlle Menu, and Yves Dartiguenave*

Laboratoire de Chimie de Coordination, 205 route de Narbonne, F31077-Toulouse, France

Francine Bélanger-Gariépy and André L. Beauchamp*

Département de Chimie, Université de Montréal, C.P.6128, Succ.A, Montréal, Québec, H3C 3J7 Canada

Received May 12, 1988

Cationic cobalt(I)–alkyne complexes $[Co(RC{\equiv}CR')(PMe_3)_3]BPh_4$ (**1a**, R = Ph, R′ = C_5H_{11}; **1b**, R = R′ = Me; **1c**, R = Ph, R′ = Me) have been synthesized from $CoBr(PMe_3)_3$. Chemical and spectroscopic properties indicate that the alkyne ligand acts as a 4e donor but remains weakly bound. Under similar experimental conditions, the electron-poor ester-substituted alkynes dimethyl acetylenedicarboxylate and methyl propiolate form in acetonitrile cobaltacyclopentadiene complexes $[\overline{CoRC{=}CR'CR'{=}C}R\text{-}(MeCN)_2(PMe_3)_2]BPh_4$ (**2a**, R = R′ = CO_2Me; **2b**, R = H, R′ = CO_2Me). Single-crystal X-ray diffraction work on **1a** ($P2_1/c$, a = 11.880 (1) Å, b = 14.629 (1) Å, c = 25.836 (3) Å, β = 90.33 (9)°, Z = 4, R = 0.055, R_w = 0.067 for 3897 reflections) confirmed the geometry deduced from spectroscopic data. The cation has a three-legged piano-stool geometry, with the alkyne unit lying in the Co–P1–C10–C11 plane and nearly parallel to the plane of the three P atoms. This structure is discussed in terms of a d^8 14e $[Co(PMe_3)_3]^+$ fragment interacting with the π-bonding alkyne. Complex stabilization by the phenyl substituents is discussed. The crystal structure of **2a** ($C2/c$, a = 41.344 (9) Å, b = 10.250 (4) Å, c = 25.377 (7) Å, β = 118.56 (2)°, Z = 8, R = 0.055, R_w = 0.061 for 3864 reflections) confirms the presence of an octahedral d^6 Co(III) monomer containing two trans phosphines, two cis acetonitriles, and a planar cobaltacyclopentadiene ring. From these results, it appears that in cationic d^8 metal complexes having two vacant $d\pi$ orbitals: (i) alkyl- and arylalkynes act as 4e donors, (ii) electron-withdrawing substituents as in dimethyl acetylenedicarboxylate or methyl propiolate are necessary to couple alkynes into cobaltacyclopentadiene complexes, and (iii) alkyne polymerization does not take place.

Introduction

Much of the current interest in the chemistry of alkynes originates in these unsaturated ligands having an important potential in organic synthesis. It is well established that their reactivity can be successfully modified by metal complexation, and this is generating increasing interest in mononuclear alkyne–metal complexes.

The binding of alkynes to metals depends on the metal configuration. Even though compounds have been reported with nearly all metals in the periodic table, there are relatively few monoalkyne complexes known.[1] Their chemistry is dominated by the presence of two filled orthogonal $\pi_\parallel$ and $\pi_\perp$ orbitals and two empty $\pi_\parallel$* and $\pi_\perp$* counterparts. Metals with d^0 to d^5 configurations in low oxidation states allow the filled $\pi_\perp$ orbital in the alkyne to encounter a suitable vacant $d\pi$ orbital in the metal, thereby giving rise to stable metal–alkyne species. Metals in configurations d^6 and higher, when coordinatively saturated, generally exhibit only weak η^2-alkyne binding because of an unfavorable two-center, four-electron repulsion between the filled alkyne $\pi_\perp$ orbital and a filled metal $d\pi$ orbital. To overcome this situation, either the alkyne acts as a two-electron ligand like an alkene or the complex loses a ligand to become coordinatively unsaturated in order to provide a vacant orbital for the filled $\pi_\perp$ alkyne orbital.

Molybdenum and tungsten in d^2, d^4, and d^6 configurations have been thoroughly studied mainly by Templeton and his group.[2-10] As for d^8 systems, interest in metal–

(1) Wilkinson, G.; Stone, F. G. A.; Abel, E. W. In *Comprehensive Organometallic Chemistry*; Pergamon: Oxford, 1982. Otsuka, S.; Nakamura, A. *Adv. Organomet. Chem.* **1976**, *14*, 245. Winlk, D. J.; Fox, J. R.; Cooper, N. J. *J. Am. Chem. Soc.* **1985**, *107*, 5012. Heck, R. F. *Organotransition Metal Chemistry*; Academic: New York, 1974.

0276-7333/89/2308-0629$01.50/0